



Published in final edited form as:

Nat Struct Mol Biol. 2011 March ; 18(3): 359–363. doi:10.1038/nsmb.1989.

The *glmS* Riboswitch Integrates Signals from Activating and Inhibitory Metabolites In Vivo

Peter Y. Watson¹ and Martha J. Fedor^{1,*}

¹Department of Chemical Physiology, Department of Molecular Biology and The Skaggs Institute for Chemical Biology, The Scripps Research Institute, 10550 North Torrey Pines Road, La Jolla, CA 92037

Abstract

The *glmS* riboswitch belongs to the family of regulatory RNAs that provide feedback regulation of metabolic genes. It is also a ribozyme that self-cleaves upon binding glucosamine-6-phosphate, the product of the enzyme encoded by *glmS*. The ligand concentration dependence of intracellular self-cleavage kinetics was measured for the first time in a yeast model system and surprisingly revealed that this riboswitch is subject to inhibition as well as activation by hexose metabolites. Reporter gene experiments in *B. subtilis* confirmed that this riboswitch integrates positive and negative chemical signals in its natural biological context. Contrary to the conventional view that a riboswitch responds to just a single cognate metabolite, our new model proposes that a single riboswitch integrates information from an array of chemical signals to modulate gene expression according to the overall metabolic state of the cell.

The *glmS* riboswitch belongs to the family of regulatory RNAs that provide feedback regulation of metabolic genes^{1–4}. Most riboswitches are found in the 5' untranslated regions of mRNAs that encode metabolic genes, where they control gene expression by adopting alternative RNA structures in the presence and absence of small ligands. Extensive studies of riboswitch interactions with cognate ligands have shown that ligand binding is associated with conformational changes that modulate gene expression by altering the availability of the Shine-Dalgarno sequence, a transcription terminator, or sites associated with RNA processing. In contrast, the *glmS* riboswitch is a ribozyme that self-cleaves upon binding glucosamine-6-phosphate, the product of the enzyme encoded by *glmS* in gram-positive bacteria^{5, 6}. Riboswitch recognition and activation by cognate metabolite ligands has been studied extensively *in vitro*, but riboswitch function amidst the complex array of intracellular metabolites with closely related structures has not been analyzed directly. GlcN6P and related compounds participate directly in *glmS* ribozyme catalysis⁷ so coenzyme-induced cleavage can be used to monitor metabolite-RNA interactions *in vivo*.

In order to understand riboswitch function in a biological context, we probed intracellular *glmS* riboswitch-ligand assembly directly and quantitatively using a system we previously

Users may view, print, copy, and download text and data-mine the content in such documents, for the purposes of academic research, subject always to the full Conditions of use:http://www.nature.com/authors/editorial_policies/license.html#terms

*Address correspondence to: Martha J. Fedor, Tel: (858) 784-2770, Fax: (858) 784-2779, mfedor@scripps.edu.

developed for studies of hairpin ribozyme folding in *Saccharomyces cerevisiae*^{8,9} (Fig. 1). The ability of exogenous glucosamine to stimulate *glmS* riboswitch self-cleavage in yeast varied during growth on different carbon sources. The patterns of self-cleavage activity observed during growth in galactose, glucose or glycerol revealed that the *glmS* riboswitch undergoes inhibition by products of hexose metabolism as well as activation by aminohexose ligands. Expression of a fluorescent reporter gene exhibited the same response to different carbon sources in *Bacillus subtilis*, the native biological context. Thus, a single ligand-binding site in the *glmS* riboswitch can integrate information from both activating and inhibitory signals *in vivo*. The ability of the *glmS* riboswitch to modulate gene expression in response to the overall metabolic state of the cell might well reflect just a single element of a complex RNA-metabolite interactome.

Results

Intracellular glucosamine dependence of riboswitch activity

We expressed the *glmS* riboswitch as a galactose-inducible chimeric mRNA in yeast, which enabled us to determine intracellular cleavage rates from their contribution to intracellular mRNA abundance and turnover kinetics^{8,9}. During yeast growth in galactose, chimeric mRNAs containing the WT *glmS* riboswitch or a riboswitch with an inactivating G33A mutation¹⁰ were expressed at similar levels (Fig. 2, Supplementary Fig. 1), indicating that the intracellular metabolite pool did not support cleavage under these growth conditions. After addition of glucosamine (GlcN), however, full length chimeric mRNA with a WT riboswitch became less abundant and RNA fragments appeared with the size expected for cleavage products (Fig. 2a,b). Exogenous GlcN did not affect the abundance of mutationally inactivated chimeric mRNA (Supplementary Fig. 1b), so exogenous GlcN clearly reduced chimeric *glmS* mRNA abundance by promoting cleavage and not by changing mRNA synthesis or turnover rates.

The cleavage rates that we calculated from decreases in the abundance of uncut chimeric *glmS* mRNA⁹ increased with increasing GlcN, as expected (Fig. 2b,c). However, the k_{max} value of 0.42 min^{-1} that we calculated from the fit to the Michaelis-Menten equation was one to two orders of magnitude lower than k_{max} values of 3 min^{-1} and 42 min^{-1} measured *in vitro* with the GlcN6P coenzyme^{5,11}. Both GlcN and GlcN6P have been implicated as coenzymes *in vitro*⁷ but GlcN6P supports 1,000 times higher activity than GlcN *in vitro*¹². GlcN taken up by yeast might activate *glmS* riboswitch cleavage directly, or it might first undergo phosphorylation to generate GlcN6P before activating the riboswitch. An active site guanine, G1, forms a hydrogen bond with the sugar phosphate of GlcN6P¹². Substitution of G1 with adenine abolishes this interaction and a *glmS* riboswitch with a G1A mutation cleaves at similar rates in GlcN and GlcN6P *in vitro*¹². We examined a chimeric mRNA with a G1A mutant riboswitch to learn how the ability to recognize the sugar phosphate affects intracellular cleavage (Fig. 2). The decrease in rates by a factor of three that we measured for the G1A mutant relative to the WT riboswitches in yeast supplemented with GlcN was much less than the 1,000-fold difference in GlcN6P-induced cleavage activity between WT and G1A riboswitches *in vitro*. WT and G1A riboswitches also exhibited similar GlcN concentration dependence in yeast, with apparent K_d^{GlcN} values in the mM

range (Fig. 2c). The similarity in intracellular self-cleavage activity between WT and G1A riboswitches suggests that GlcN directly promotes riboswitch self-cleavage in yeast.

The increase in intracellular cleavage rates with increasing exogenous GlcN concentrations reached a plateau near 100 mM GlcN (Fig. 2c). This plateau is not likely to reflect saturation of import or activation of GlcN catabolism, since intracellular GlcN concentrations continue to increase in yeast as media concentrations of GlcN increase up to 7% (w/v) (400 mM)¹³. Moreover, the $K_{d,app}^{GlcN}$ value of 23 mM measured *in vivo* is not significantly different from the $K_{d,app}^{GlcN}$ value of 38 mM measured *in vitro* under conditions designed to approximate the intracellular ionic environment (Fig. 2d). Thus, the apparent K_d values measured for both the WT and G1A riboswitches *in vivo* appear to reflect their affinity for GlcN.

Dependence of riboswitch activity on carbon metabolism

Many riboswitches must assemble into ligand-bound structures during transcription, since gene regulation often depends on transcription terminator or anti-terminator structures^{2–4}. However, some riboswitches alter splicing efficiency or ribosome binding, which would not require co-transcriptional ligand binding. A possible requirement for co-transcriptional folding of ligand-bound RNA is an important aspect of ligand recognition and riboswitch function that had not yet been studied *in vivo*. To learn if ligand binding must occur during *glmS* riboswitch transcription *in vivo*, GlcN was added after transcription was inhibited by transfer of yeast into media containing glucose instead of galactose (Fig. 3a). Chimeric mRNA with the WT ribozyme and the mutationally inactivated G33A ribozyme decayed at the same rates after GlcN addition, suggesting that GlcN did not activate cleavage after transcription inhibition.

However, this evidence that GlcN did not induce cleavage of the fully transcribed riboswitch was surprising since *glmS* riboswitches fold into virtually identical structures in the presence and absence of ligand *in vitro*^{14,15}, so we considered an alternative explanation. A physiological role for riboswitch inhibition has not been considered previously, but glucose-6-phosphate (Glc6P) is a competitive inhibitor of *glmS* riboswitch cleavage *in vitro*⁷. Growth in glucose increases intracellular concentrations of Glc6P¹⁶, raising the intriguing possibility that the absence of detectable *glmS* riboswitch cleavage activity after transfer of yeast into glucose media results from competitive inhibition of cleavage by glucose metabolites *in vivo*.

Glc6P is an intermediate in the metabolism of both galactose and glucose¹⁷ but glycerol metabolism does not proceed through any hexose phosphate intermediates that are likely to interact with the *glmS* riboswitch¹⁸. In striking contrast to the absence of cleavage in glucose media, riboswitch cleavage products appeared and WT chimeric mRNA decay accelerated relative to decay of the inactive G33A mutant upon GlcN addition when transcription was inhibited by transfer into glycerol rather than glucose (Fig. 3b). Thus, GlcN binding and cleavage did occur in full-length chimeric mRNAs even after transcription inhibition, but only during a glycerol chase. This evidence that GlcN induces *glmS* riboswitch cleavage activity after transcription inhibition in glycerol suggests that the failure of GlcN to induce cleavage in glucose did not reflect a requirement for co-transcriptional folding of a ligand

complex, but rather differences in the metabolic state of the cell during growth in glycerol versus glucose.

Furthermore, cleavage occurred in the absence of exogenous GlcN during mRNA decay in glycerol (Fig. 3b), but not during steady-state growth in media with galactose (Fig. 2) or during decay in glucose (Fig 3a). Thus, differences in riboswitch activity during growth in glycerol relative to growth in galactose or glucose did not reflect differences in uptake of exogenous GlcN and must reflect differences in the intracellular concentrations of endogenous activating and inhibitory metabolites during growth in different carbon sources. These differences in riboswitch activity during growth in glycerol, galactose and glucose provide strong evidence that products of hexose metabolism, such as Glc6P, inhibit cleavage by competing with activating ligands for riboswitch binding. We measured a $K_{i,app}$ of 10 mM for Glc6P inhibition of GlcN-mediated self-cleavage *in vitro* in reactions designed to approximate intracellular conditions (Fig. 4a). A similar inhibition constant of 3 mM has been reported for Glc6P inhibition of GlcN6P-activated *glmS* riboswitch self-cleavage *in vitro*⁹. We attempted to measure intracellular concentrations of activating and inhibitory metabolites, but could not resolve hexose and aminohexose isomers. However, the intracellular Glc6P concentration of about 2.3 mM reported for yeast grown in glucose¹⁹ is on the same order as the inhibition constants measured *in vitro*, consistent with an inhibitory role for Glc6P in gene regulation by the *glmS* riboswitch *in vivo*. Thus, the *glmS* riboswitch responds to a complex array of both positive and negative signals that arise from carbon metabolism as yeast grow in different environments.

We validated the biological significance of this finding using green fluorescent protein (GFP) reporter constructs in which riboswitch cleavage reduces fluorescence in *B. subtilis*. Fluorescence intensity decreased significantly in bacteria with a WT riboswitch reporter grown in media with GlcN relative to reporter mRNA with an inactivating G33A mutation (Fig. 4b), as expected if GlcN-activated self-cleavage reduced reporter mRNA abundance. Furthermore, *B. subtilis* exhibited enhanced fluorescence during growth in media with both GlcN and glucose, consistent with inhibition of *glmS* riboswitch self-cleavage by glucose metabolites. The difference in fluorescence did not reflect metabolic conversion of glucose to GlcN because we used a *glmS*⁻ strain²⁰. Furthermore, no increase in fluorescence occurred in bacteria expressing a reporter with a mutationally inactivated G33A riboswitch, so it did not reflect changes in mRNA synthesis or turnover. Thus, the *glmS* riboswitch was subject to inhibition by glucose-derived metabolites in gram-positive bacteria, its natural biological context. These results provide the first evidence that metabolites play both stimulatory and inhibitory roles in riboswitch-mediated gene regulation *in vivo*.

Discussion

Large, unexpected changes in self-cleavage kinetics under different growth conditions revealed inhibition as well as activation by hexose metabolites. Reporter gene experiments in *B. subtilis* confirmed that the *glmS* riboswitch integrates positive and negative chemical signals in its natural biological context. These findings demonstrate that *glmS* riboswitch activity depends not only on the concentration of cognate ligands that promote self-cleavage but also on products of hexose metabolism that inhibit self-cleavage. The ability of

intracellular metabolites to block the interaction between a riboswitch and its cognate ligand points to an unanticipated role for riboswitches in integration of multiple chemical signals. Negative feedback regulation of GlmS through riboswitch activation by intracellular GlcN6P is well known^{5,6}. However, our findings provide the first evidence that intracellular products of hexose metabolism block activation by cognate ligands, thereby enabling the *glmS* riboswitch to modulate gene expression in response to the overall metabolic state of the cell. A previous report that growth of *B. subtilis* in GlcN reduces GlmS activity, but growth in glucose and GlcN does not²¹, supports the idea that the riboswitch integrates information from an array of metabolites, not just its cognate ligand. NagB deaminates GlcN6P to generate fructose-6-phosphate, the reverse of the reaction catalyzed by GlmS. NagB is downregulated in glucose and upregulated in GlcN^{21,22}. Intriguingly, our results indicate that the *glmS* riboswitch plays a role in reciprocal regulation of GlmS, responding to intracellular hexose and aminohexose metabolites to achieve both feed-forward upregulation and feedback downregulation of GlmS expression (Fig. 5).

These findings have broad implications for mechanisms of riboswitch-mediated gene regulation. Tandem riboswitch arrangements have been shown to respond to multiple metabolites²³ but this is the first evidence that a single riboswitch responds to multiple chemical signals, both activating and inhibitory. The ability of a single riboswitch to integrate information from multiple chemical signals may well extend to other riboswitches. The SAM-I riboswitch, which regulates ratios of S-Adenosylmethionine (SAM) to S-adenosyl-L-homocysteine (SAH)^{1,24}, provides one illustration. The P1 and P3 helices of the SAM-I riboswitch interact with different functional groups of SAM to stabilize a specific tertiary structure and promote folding of a transcription terminator. SAH forms the same interaction with the P3 helix as SAM but lacks a key interaction with the P1 helix^{24,25}. If the SAM riboswitch integrates positive and negative chemical signals like the *glmS* riboswitch, abundant SAH might compete with SAM for P3 binding without stabilizing the interhelical tertiary structure or promoting folding of the transcription terminator. Indeed, SAM-I riboswitch variants with similar affinities for SAM *in vitro* have different effects on downstream genes *in vivo*, which might reflect different susceptibilities to inhibition by SAH or related metabolites *in vivo*²⁶. Thus, the SAM-I riboswitch might integrate information about SAM and SAH abundance in the same way that the *glmS* riboswitch integrates information from carbon metabolism.

We found that the *glmS* riboswitch responds to both inhibitory and activating metabolites in yeast and bacteria. Our finding that *glmS* riboswitch activity is modulated by several metabolites *in vivo*, not just a single cognate ligand, suggests an expanded physiological role for regulatory RNAs in integrating information from an array of chemical signals. We propose a new paradigm for riboswitch-mediated gene regulation in which ligand binding reflects the concentrations and affinities of an array of chemical signals and serves to integrate information about the metabolic state of the cell. The *glmS* riboswitch response to multiple metabolites that we describe here likely represents an early indication of a vast RNA-metabolite interactome that remains to be explored.

Methods

Plasmid construction and propagation

Oligonucleotide primer sequences are shown in Supplementary Table 1. A plasmid template for transcription of the *glmS* ribozyme, pTS, was created by fusing the ribozyme sequence from *B. anthracis* to a T7 RNA polymerase promoter, introducing flanking BamH I and EcoR I sites using PCR, and insertion into pUC18²⁷. The *glmS* ribozyme sequence was inserted into the 3' UTR of the yeast *PGK1* gene in pGS, a derivative of pRS316²⁸, for expression of chimeric *glmS PGK1* mRNAs in yeast. pGS was prepared from pAMGAL28, a plasmid previously used for galactose-inducible expression of chimeric hairpin ribozyme mRNAs in yeast^{8,28,29}. To construct pGS, an Mlu I site was inserted upstream of the ribozyme sequence in pTS using QuikChangeTM mutagenesis (Stratagene) and an Afl II-Mlu I fragment encoding the *glmS* ribozyme was inserted into the 3' UTR of the *PGK1* gene.

The plasmid template for transcription of hybridization probes, pGAP, contained sequences corresponding to an Nhe I and Bgl II fragment of yeast ACT1 mRNA and chimeric *glmS PGK1* mRNA. pGAP was derived from pGEM4-Z using conventional procedures as described previously²⁸.

pBGSEF, a derivative of pAD43-25³⁰ (Bacillus Genetic Stock Center) that contains the complete *glmS* 5' UTR fused to a GFP coding sequence was constructed to express GFP under *glmS* ribozyme control in *B. subtilis*. A fragment containing the complete 5' UTR and the *glmS* ribozyme coding sequence from *B. anthracis* was inserted into pAD43-25 using QuikChangeTM mutagenesis³¹. G1A and G33A mutations were introduced into pTS, pGAP, pGS, and pBGSEF using QuikChangeTM mutagenesis. Plasmids were propagated in *E. coli* strains XL1-Blue or XL10-Gold (Stratagene), *S. cerevisiae* strain HFY114 (*MATa ade2-1 his3-11,15 leu2-3 112 trp1-1 ura3-1 can1-100*)³², or *B. subtilis* strain 60984 (*glmS2 metC7 trpC2*)²⁰ (Bacillus Genetic Stock Center)

Intracellular self-cleavage kinetics

Intracellular cleavage assays were performed as previously described⁹, except that minimal galactose media was maintained at pH 7 using phosphate buffer (50mM PO₄). Glucosamine (pH 7.0, 30°C) was added at the indicated concentrations, and cultures were incubated for 1 hr at 30 °C before extracting RNA. Intracellular cleavage rates can be calculated from the relative abundance of WT and mutationally inactivated chimeric mRNAs at steady state^{8,28,29}. Reported values represent the mean, and errors bars represent the standard deviation, of two or more experiments. Cleavage rates were fit to the Michaelis-Menten equation, and reported kinetic parameters represent the constants and errors of the fit.

Time course experiments for measuring chimeric mRNA decay kinetics were initiated by transferring yeast cultures from minimal media with 2% (w/v) galactose to minimal media with either 2% (w/v) glucose or 3% (v/v) glycerol. Chimeric mRNAs were quantified using RNase protection assays and normalized with respect to yeast *ACT1* mRNA, as described⁹. Intracellular chimeric mRNA decay rates were calculated from the fit to a single exponential rate equation. Intracellular cleavage rates were calculated from the difference between decay rates of chimeric mRNAs with a WT riboswitch insert or a riboswitch insert with an

inactivating G33A mutation. The plots shown in the figures represent typical decay time course experiments. Reported values represent the mean and standard deviation of two or more experiments.

In vitro cleavage kinetics

³²P-labeled WT and G1A riboswitch RNAs were transcribed from linearized pTS and pTSG1A plasmids using T7 RNA polymerase and [α -³²P ATP] as described³³, except that reactions contained 20 mM NaHEPES pH 7.8 instead of TrisCl, which promotes *glmS* riboswitch cleavage⁷. Transcripts were fractionated by denaturing gel electrophoresis and eluted. Full-length riboswitch RNAs were converted into sodium salts by DEAE-650M chromatography (Toyopearl), precipitated with ethanol and dissolved in 50 mM NaHEPES pH 7.5.

To measure kinetic parameters for GlcN-activated self-cleavage, RNA solutions were heated to 85 °C for 1 min., cooled to 30 °C, and brought to final concentrations of 50 mM NaHEPES pH 7.5, 2 mM MgCl₂, 150 mM NaCl, and 0.1 mM EDTA. GlcN (pH 7.5) was added to reach the indicated concentrations. Aliquots were removed at intervals over one hour, quenched by the addition of 90% (v/v) formamide, 25 mM EDTA, 0.002% (w/v) xylene cyanole and 0.002% (w/v) bromophenol blue, and fractionated by denaturing gel electrophoresis. Cleavage rates were calculated from the fit to a single exponential rate equation³⁴. $K_{d,app}^{GlcN}$ values were calculated from the fit to $K_{d,app}^{GlcN} = k_{max} \times [GlcN] / ([GlcN] + K_{d,app})$. Reported values represent the mean and standard deviation from three experiments.

Inhibition constants were determined from cleavage rates measured in reactions with 5 mM GlcN and the indicated concentrations of Glc6P. The IC₅₀^{Glc6P} was calculated from the fit to a sigmoid curve: $k_{cleavage} = k_{min} + (k_{max}) / (1 + e^{((K_i - [Glc6P]) * C)})$, where C is the slope of the Hill plot of [Glc6P] versus $k_{obs,cleavage}$. The $K_{i,app}$ was calculated using the Cheng-Prusoff equation³⁵ and the $K_{d,app}^{GlcN}$ value measured under the same conditions.

GFP fluorescence in *B. subtilis*

B. subtilis was transformed³⁶ with plasmids encoding WTGFP or G33AGFP riboswitch-GFP fusion proteins. We used *B. subtilis* strain 60984, which has a *glmS2* mutation that prevents synthesis of GlcN6P from glucose to facilitate manipulation of intracellular hexose and aminohexose metabolite concentrations. Cells were grown overnight with agitation at 37 °C in minimal media supplemented with 0.5% (w/v) GlcN, pelleted by centrifugation then resuspended in minimal media with 0.5% (w/v) glucose or 0.5% (w/v) GlcN as indicated, to an absorbance at 600 nm (A_{600}) of 0.05 or lower. Cells were grown at 37 °C to mid log phase ($A_{600} \sim 0.3$), pelleted, resuspended in fresh media containing the same concentrations of glucose and GlcN to obtain an $A_{600} = 0.15$, and grown again to mid-log phase ($A_{600} \sim 0.3$). Samples (20 μ L) were transferred into a 384-well black microplate (Greiner), excited at 460 nm, and emission intensity was measured at 511 nm in a SpectraMax M2e fluorescent plate reader (Molecular Devices). Emission intensity was normalized to the absorbance at 600 nm of each sample, and background emission from untransformed cells was subtracted.

Reported data represent the mean and standard deviation of fluorescence emission intensity obtained from six replicate experiments.

Supplementary Material

Refer to Web version on PubMed Central for supplementary material.

Acknowledgments

This work was supported by NIH Grant RO1 GM062277. P.Y. Watson was supported by a graduate fellowship from The Skaggs Institute for Chemical Biology. We thank Joseph Pogliano for advice regarding the *B. subtilis* experiments, Julia Viladoms and Manami Saha for assistance with plasmid constructions, and JV for critical reading of the manuscript.

References

1. Montange RK, Batey RT. Riboswitches: emerging themes in RNA structure and function. *Annu Rev Biophys Biomol Struct.* 2008; 37:117–133.
2. Henkin TM. Riboswitch RNAs: using RNA to sense cellular metabolism. *Genes Dev.* 2008; 22:3383–3390. [PubMed: 19141470]
3. Roth A, Breaker RR. The structural and functional diversity of metabolite-binding riboswitches. *Annu Rev Biochem.* 2009; 78:305–334. [PubMed: 19298181]
4. Dambach MD, Winkler WC. Expanding roles for metabolite-sensing regulatory RNAs. *Curr Opin Microbiol.* 2009; 12:161–169. [PubMed: 19250859]
5. Winkler WC, Nahvi A, Roth A, Collins JA, Breaker RR. Control of gene expression by a natural metabolite-responsive ribozyme. *Nature.* 2004; 428:281–286. [PubMed: 15029187]
6. Collins JA, Irnov I, Baker S, Winkler WC. Mechanism of mRNA destabilization by the glmS ribozyme. *Genes Dev.* 2007; 21:3356–3368. [PubMed: 18079181]
7. McCarthy TJ, et al. Ligand requirements for glmS ribozyme self-cleavage. *Chem Biol.* 2005; 12:1221–1226. [PubMed: 16298301]
8. Donahue CP, Fedor MJ. Kinetics of hairpin ribozyme cleavage in yeast. *RNA.* 1997; 3:961–973. [PubMed: 9292496]
9. Watson, P.Y.; Fedor, M.J. *Meth Enzymol, Biophysical, Chemical, and Functional Probes of RNA Structure, Interactions and Folding, Pt A. Vol. 468.* Elsevier Academic Press Inc; San Diego: 2009. Determination of intracellular RNA folding rates using self-cleaving RNAs; p. 259–286.
10. Klein DJ, Been MD, Ferré-D'Amaré AR. Essential role of an active-site guanine in glmS ribozyme catalysis. *J Am Chem Soc.* 2007; 129:14858–14859. [PubMed: 17990888]
11. Cochrane JC, Lipchick SV, Smith KD, Strobel SA. Structural and chemical basis for glucosamine 6-phosphate binding and activation of the glmS ribozyme. *Biochemistry.* 2009; 48:3239–3246. [PubMed: 19228039]
12. Klein DJ, Wilkinson SR, Been MD, Ferré-D'Amaré AR. Requirement of helix P2.2 and nucleotide G1 for positioning the cleavage site and cofactor of the glmS ribozyme. *J Mol Biol.* 2007; 373:178–189. [PubMed: 17804015]
13. Burger M, Hejmová L. Uptake of metabolizable sugars by *Saccharomyces cerevisiae*. *Folia Biol (Krakow).* 1961; 6:80–85.
14. Klein DJ, Ferré-D'Amaré AR. Structural basis of glmS ribozyme activation by glucosamine-6-phosphate. *Science.* 2006; 313:1752–1756. [PubMed: 16990543]
15. Cochrane JC, Lipchick SV, Strobel SA. Structural investigation of the glmS ribozyme bound to its catalytic cofactor. *Chem Biol.* 2007; 14:97–105. [PubMed: 17196404]
16. Rizzi M, et al. In vivo investigations of glucose transport in *Saccharomyces cerevisiae*. *Biotechnol Bioeng.* 1996; 49:316–327. [PubMed: 18623583]

17. Sellick CA, Campbell RN, Reece RJ. Galactose metabolism in yeast-Structure and regulation of the Leloir pathway enzymes and the genes encoding them. *Int Rev Cell Molec Biol.* 2008; 269:111–150. [PubMed: 18779058]
18. Nevoigt E, Stahl U. Osmoregulation and glycerol metabolism in the yeast *Saccharomyces cerevisiae*. *FEMS Microbiol Rev.* 1997; 21:231–241. [PubMed: 9451815]
19. Albe KR, Butler MH, Wright BE. Cellular concentrations of enzymes and their substrates. *J Theor Biol.* 1990; 143:163–195. [PubMed: 2200929]
20. Freese EB, Cole RM, Klofat W, Freese E. Growth, sporulation, and enzyme defects of glucosamine mutants of *Bacillus subtilis*. *J Bacteriol.* 1970; 101:1046–1062. [PubMed: 4985585]
21. Bates C, Pasternak CA. Further studies on the regulation of amino sugar metabolism in *Bacillus subtilis*. *Biochem J.* 1965; 96:147–154. [PubMed: 14343123]
22. Blencke HM, et al. Transcriptional profiling of gene expression in response to glucose in *Bacillus subtilis*: regulation of the central metabolic pathways. *Metab Eng.* 2003; 5:133–149. [PubMed: 12850135]
23. Sudarsan N, et al. Tandem riboswitch architectures exhibit complex gene control functions. *Science.* 2006; 314:300–304. [PubMed: 17038623]
24. Montange RK, et al. Discrimination between closely related cellular metabolites by the SAM-I riboswitch. *J Mol Biol.* 396:761–772. [PubMed: 20006621]
25. Montange RK, Batey RT. Structure of the S-adenosylmethionine riboswitch regulatory mRNA element. *Nature.* 2006; 441:1172–1175. [PubMed: 16810258]
26. Tomsic J, McDaniel BA, Grundy FJ, Henkin TM. Natural variability in S-adenosylmethionine (SAM)-dependent riboswitches: S-box elements in *Bacillus subtilis* exhibit differential sensitivity to SAM *In vivo* and *in vitro*. *J Bacteriol.* 2008; 190:823–833. [PubMed: 18039762]
27. Norrander J, Kempe T, Messing J. Construction of improved M13 vectors using oligodeoxynucleotide-directed mutagenesis. *Gene.* 1983; 26:101–106. [PubMed: 6323249]
28. Donahue CP, Yadava RS, Nesbitt SM, Fedor MJ. The kinetic mechanism of the hairpin ribozyme *in vivo*: influence of RNA helix stability on intracellular cleavage kinetics. *J Mol Biol.* 2000; 295:693–707. [PubMed: 10623557]
29. Sikorski RS, Hieter P. A system of shuttle vectors and yeast host strains designed for efficient manipulation of DNA in *Saccharomyces cerevisiae*. *Genetics.* 1989; 122:19–27. [PubMed: 2659436]
30. Dunn AK, Handelsman J. A vector for promoter trapping in *Bacillus cereus*. *Gene.* 1999; 226:297–305. [PubMed: 9931504]
31. Geiser M, Cebe R, Drewello D, Schmitz R. Integration of PCR fragments at any specific site within cloning vectors without the use of restriction enzymes and DNA ligase. *Biotechniques.* 2001; 31:88–90. 92. [PubMed: 11464525]
32. He, F.; Amrani, N.; Johansson, MJO.; Jacobson, A. RNA Turnover in Eukaryotes: Analysis of Specialized and Quality Control RNA Decay Pathways. Vol. 449. Elsevier Academic Press Inc; San Diego: 2008. Qualitative and quantitative assessment of the activity of the yeast nonsense-mediated mRNA decay pathway; p. 127–147.
33. Milligan JF, Uhlenbeck OC. Synthesis of small RNAs using T7 RNA polymerase. *Methods Enzymol.* 1989; 180:51–62. [PubMed: 2482430]
34. Long DM, Uhlenbeck OC. Kinetic characterization of intramolecular and intermolecular hammerhead RNAs with stem II deletions. *Proc Natl Acad Sci.* 1994; 91:6977–6981. [PubMed: 7518924]
35. Cheng Y, Prusoff WH. Relationship between the inhibition constant (K₁) and the concentration of inhibitor which causes 50 per cent inhibition (I₅₀) of an enzymatic reaction. *Biochem Pharmacol.* 1973; 22:3099–3108. [PubMed: 4202581]
36. Anagnostopoulos C, Spizizen J. Requirements for transformation in *Bacillus subtilis*. *J Bacteriol.* 1961; 81:741–746. [PubMed: 16561900]
37. Wilkinson SR, Been MD. A pseudoknot in the 3' non-core region of the glmS ribozyme enhances self-cleavage activity. *RNA.* 2005; 11:1788–1794. [PubMed: 16314452]

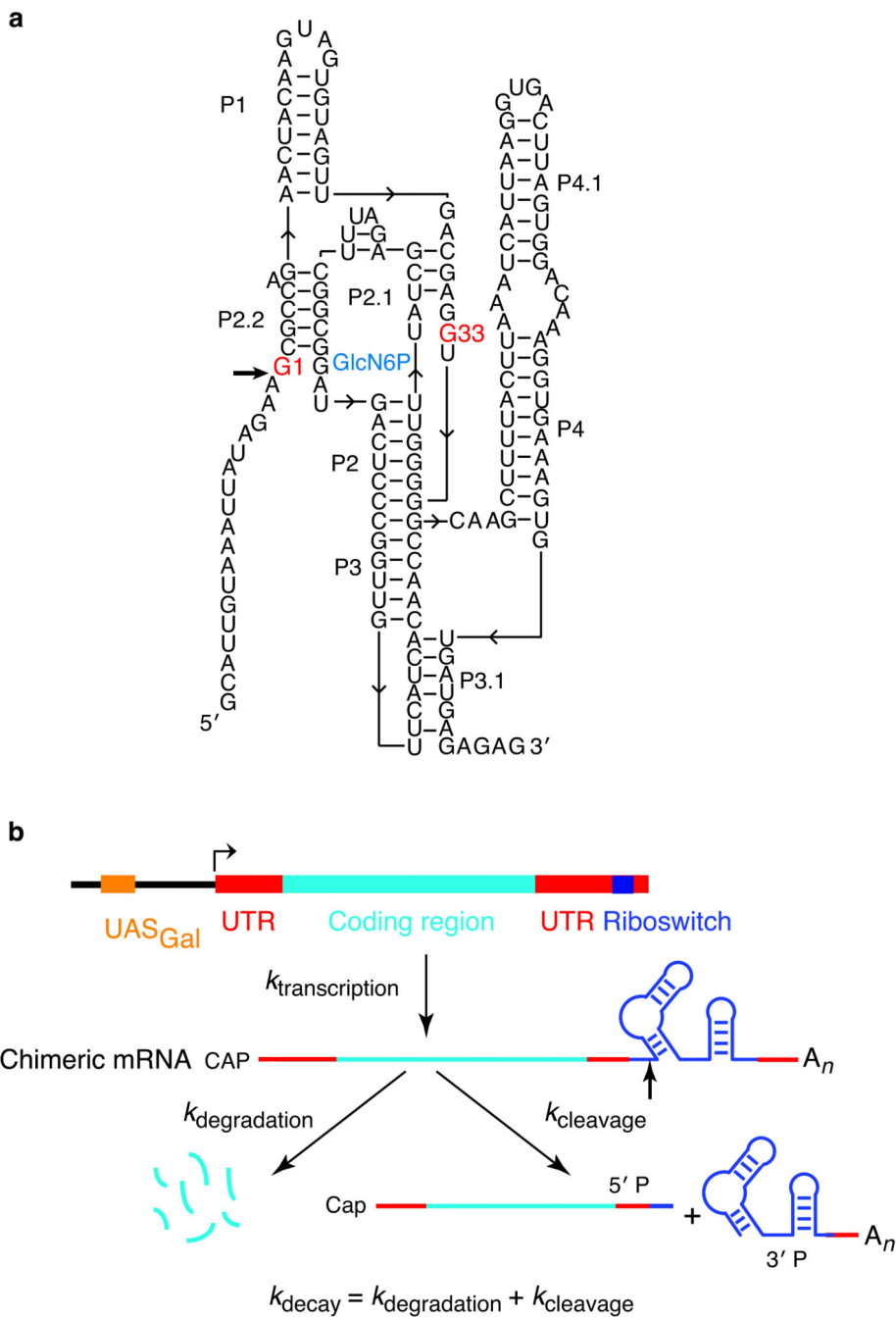


Figure 1. System for measuring intracellular *glmS* riboswitch cleavage kinetics. **(a)** The *glmS* riboswitch from *B. anthracis*³⁷. Cleavage at the site indicated by the arrow yields 5' product (5' P) and 3' product (3' P) RNAs. **(b)** The riboswitch coding sequence was inserted into the 3' UTR of the yeast *PGK1* gene and expressed under the control of a galactose inducible promoter. Full-length *glmS* chimeric mRNA with a WT riboswitch decays faster than an mRNA with an inactivating G33A mutation¹⁰ and is less abundant at steady state due to the contribution of cleavage to decay kinetics⁹. Comparison of chimeric mRNAs with a WT

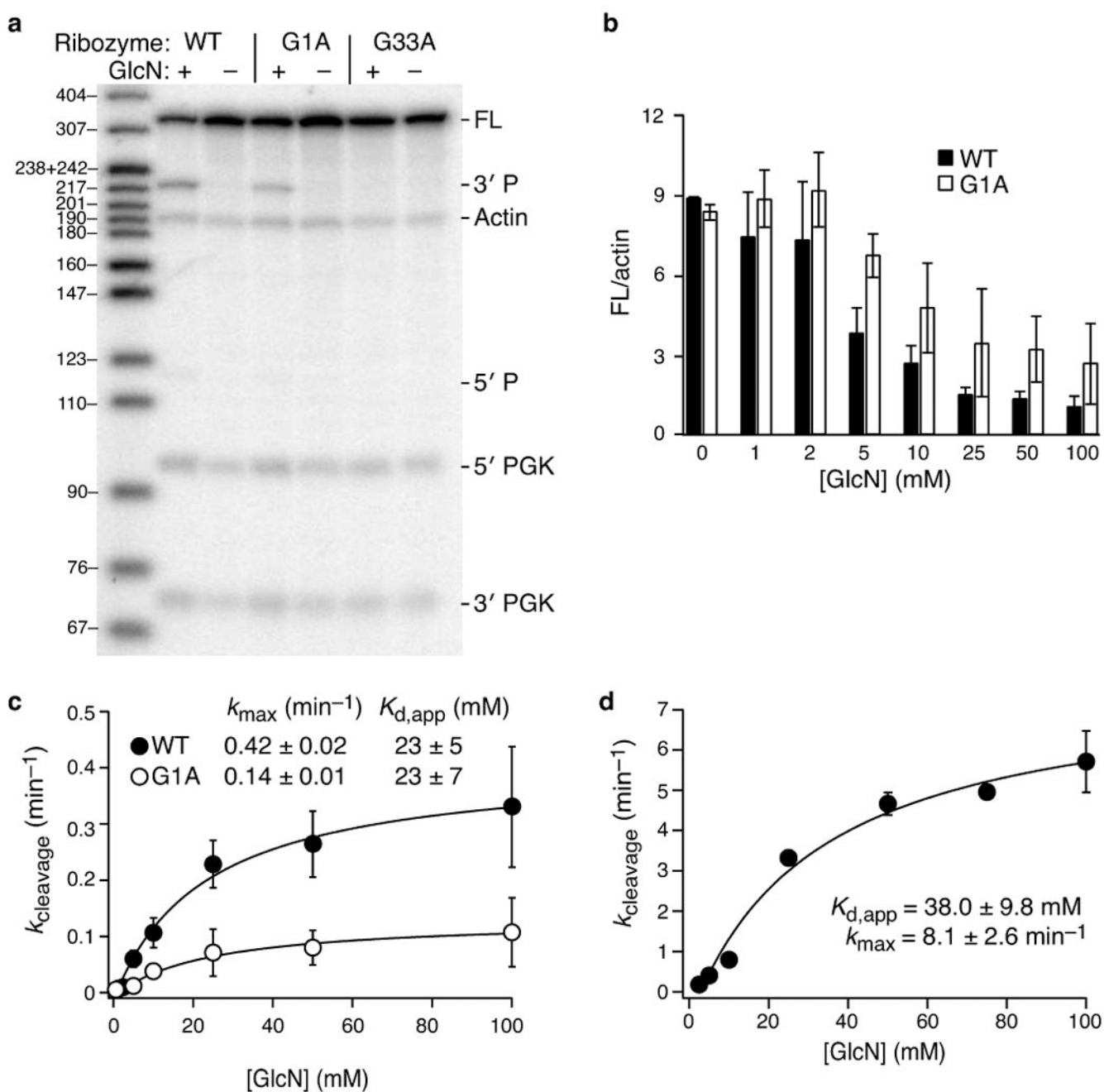
riboswitch to mRNA with the inactivating G33A mutation ensures that changes in decay kinetics reflect cleavage and not an effect of the sequence insertion on mRNA stability.

Author Manuscript

Author Manuscript

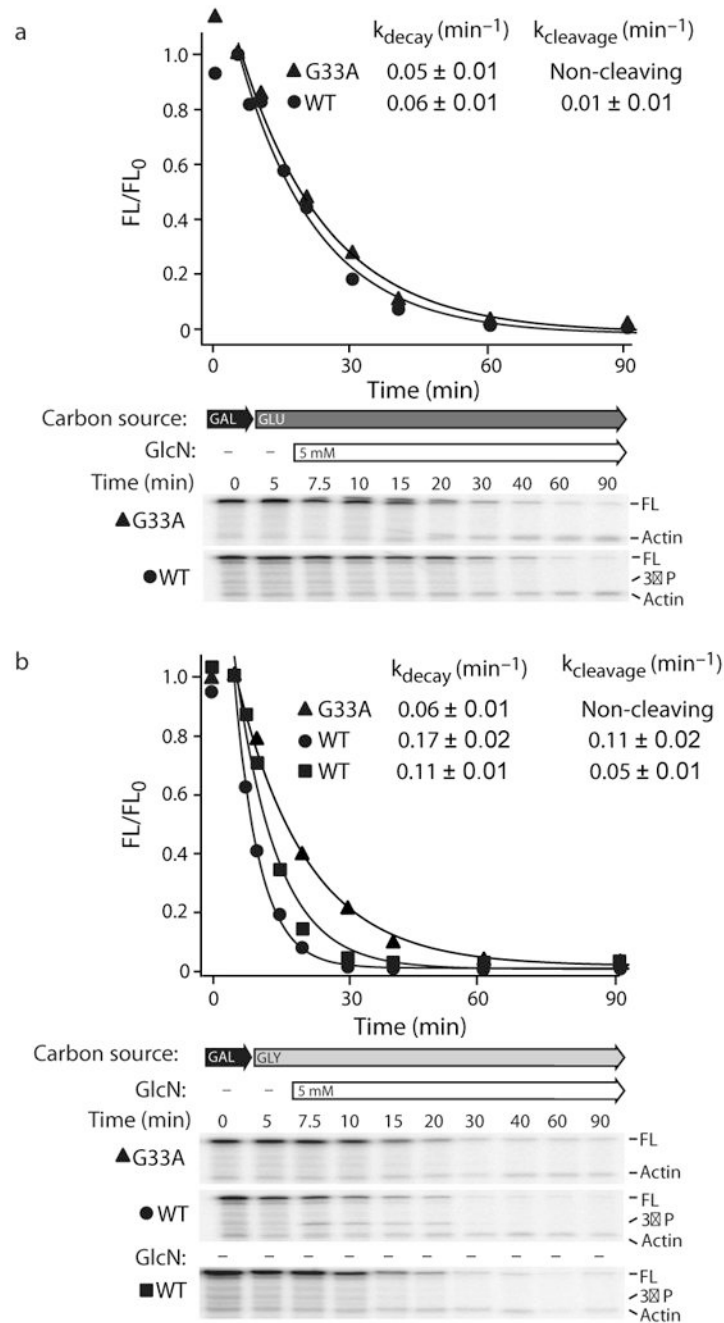
Author Manuscript

Author Manuscript

**Figure 2.**

GlcN dependence of *glmS* riboswitch cleavage in yeast. **(a)** RNase protection assays revealed full-length (336 nt) and 5' P and 3' P cleavage product RNAs (121 and 215 nt respectively) in yeast expressing WT and G1A chimeric mRNAs during growth in media with galactose and 10 mM GlcN along with RNA fragments upstream and downstream of the riboswitch insert in genomic *PGK1* mRNA (93 and 70 nt, respectively). Only full-length mRNA was detected in yeast expressing the mutationally inactivated G33A riboswitch. *Act1* mRNA (191 nt) was used for normalization. **(b)** Lower abundance of full-length chimeric mRNAs with WT and G1A riboswitch insertions relative to chimeric mRNA with an

inactivating G33A mutation during growth in galactose and different GlcN concentrations reflects GlcN-dependent cleavage. Bars represent the mean and error bars represent the standard deviation of two or more experiments. **(c)** Intracellular cleavage rates were calculated from the steady state abundance⁹ of chimeric mRNAs with WT or G1A riboswitch inserts and fit to the Michaelis-Menten equation to calculate apparent K_d^{GlcN} values. Points represent the mean and error bars represent the standard deviations of rates calculated from the data shown in (b). **(d)** GlcN dependence of *glmS* riboswitch cleavage kinetics measured under conditions that approximate a physiological ionic environment *in vitro*. The plot shows rates measured in a representative experiment and error bars represent the standard error of the fit. Reported k_{max} and $K_{d,app}^{\text{GlcN}}$ values represent the mean and standard deviation of values obtained from three or more experiments.

**Figure 3.**

Chimeric mRNA cleavage and decay kinetics after transcription inhibition in different carbon sources. **(a)** WT and G33A chimeric mRNA exhibited similar decay rates after transcription inhibition by transfer of yeast from galactose to glucose with 5 mM GlcN. **(b)** WT chimeric mRNA exhibited faster decay than chimeric mRNA with an inactivating G33A mutation after transcription inhibition in glycerol, reflecting the contribution of riboswitch cleavage. Cleavage rates were calculated from the difference between the decay rate of full-length chimeric mRNA with a G33A riboswitch insert, which reflects degradation through

the endogenous mRNA turnover pathway, and chimeric mRNA with a WT riboswitch insert, which decays through both cleavage and normal degradation pathways⁹. Addition of 5 mM GlcN after transcription inhibition accelerated decay of chimeric mRNA with a WT riboswitch even further. Decay kinetics for G33A mutant chimeric were the same under all conditions for which WT decay rates are reported, indicating that mRNA turnover through endogenous mRNA turnover pathways was not affected by riboswitch insertions or changes carbon sources. Reported rates represent the mean and standard deviation of values obtained from two or more replicate experiments.

Author Manuscript

Author Manuscript

Author Manuscript

Author Manuscript

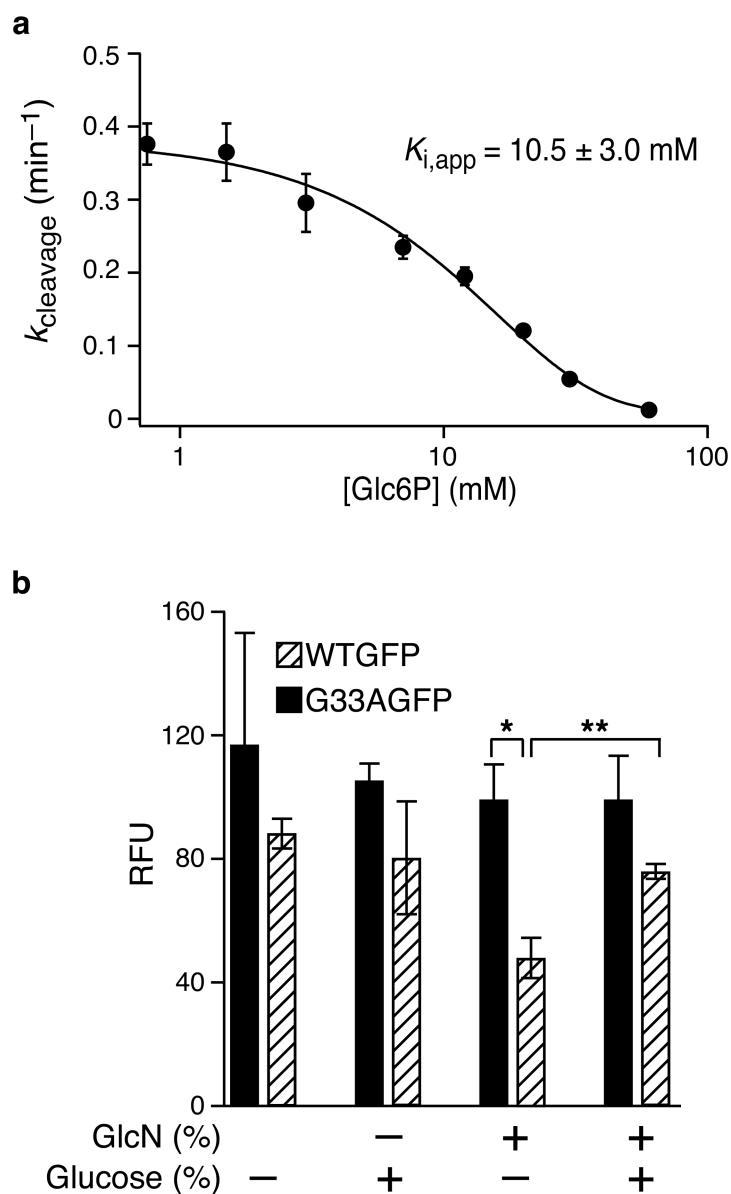


Figure 4.

Hexoses inhibit riboswitch cleavage *in vitro* and in *B. subtilis*. **(a)** Cleavage rates were measured in 5mM GlcN and varying concentrations of Glc6P under conditions that approximate a physiological ionic environment *in vitro*. The plot shows rates measured in a representative experiment and error bars represent the standard error of the fit. The reported $K_{i,\text{app}}^{\text{Glc6P}}$ values represent the mean and standard deviation of values obtained from two or more experiments. **(b)** Riboswitch activity in *B. subtilis* with a GFP-coding sequence fused to the WT (WTGFP) or inactive (G33AGFP) riboswitch. WTGFP showed a significant (*p<0.001) reduction in fluorescence intensity relative to G33AGFP during growth in minimal media with GlcN, indicating that cleavage decreased GFP mRNA abundance, as expected. Fluorescence intensity increased significantly in bacteria with WTGFP (**p<0.005) in media with glucose and GlcN, but did not change in bacteria with G33AGFP

($p > 0.3$), evidence that glucose or a glucose-derived metabolite prevented riboswitch cleavage from reducing WTGFP mRNA abundance. Bars represent the mean and standard deviation of fluorescence emission intensity obtained from six replicate experiments. Statistical significance was determined using a one-tailed Student's *t*-test.

Author Manuscript

Author Manuscript

Author Manuscript

Author Manuscript

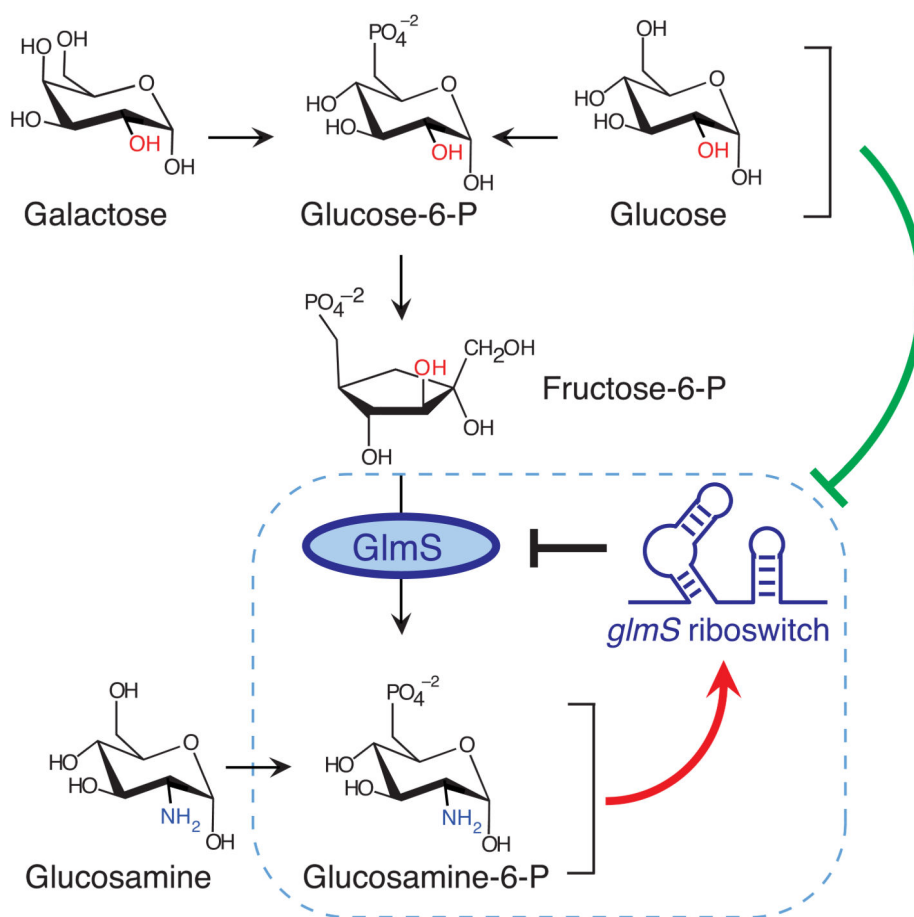


Figure 5.

Model for riboswitch regulation of GlmS gene expression. Riboswitch cleavage activity integrates information about the metabolic state of the cell by responding to the concentrations and affinities of an array of chemical signals. In this model, hexoses increase *glmS* mRNA abundance and upregulate GlmS expression by inhibiting riboswitch cleavage (green line), while aminohexoses decrease *glmS* mRNA abundance and downregulate GlmS expression by activating riboswitch cleavage (red line). The dashed box illustrates the former model that a single cognate ligand, GlcN6P, activates the riboswitch to downregulate GlmS expression.